Analysis of a Simplified Hopping Robot

A paper submitted to the
International Journal of Robotics Research

Daniel E. Koditschek and Martin Bühler [1]

Center for Systems Science
Yale University, Department of Electrical Engineering

May 20, 1988

[1]This work is supported in part by the National Science Foundation under grant No. DMC-8552851, a Presidential Young Investigator Award held by the first author.

Abstract

We offer some preliminary analytical results concerning simplified models of Raibert's hopper. We represent the task of achieving a recurring hopping height for an actuated "ball" robot as a stability problem in the setting of a nonlinear discrete dynamical system. We model the properties of Raibert's control scheme in a simplified fashion, and provide conditions under which the procedure results in closed loop dynamics possessed of a globally attracting fixed point — the formal rendering of what we intuitively mean by a "correct" strategy. The motivation for this work is the hope that it will facilitate the development of general design principles for "dynamically dexterous" robots.

1 Introduction

This paper presents a preliminary analysis of the limiting behavior of a "hopping ball" controlled by sensory feedback to achieve a stable periodic motion in the earth's gravitational field. We take as inspiration and as point of departure, the pioneering work of Marc Raibert whose successful implementation of simple yet appropriate control procedures has resulted in working physical prototypes of stable hopping, running, and cantering gaits [5]. The most striking feature of these control algorithms is their minimal dependence on "higher level" intelligence and elegant reliance upon the intrinsic physical characteristics of actuators and masses. An understanding of the capabilities and limits of such approaches to robot task specification and control seems essential to the reliable construction of "dynamically dexterous robots" in general.

This last phrase we understand to mean the problem of robotic interaction with incompletely actuated environments (i.e., the absence of a continuous control input at every degree of mechanical freedom) whose dynamical structure changes in response to the robot's actions. In our understanding, there are (at least) three significant directions of inquiry in the exploration of any robotic task domain. The first is a formal representation of the environment, and a formal "encoding" of the specified tasks within that representation. The second is the construction of control laws along with a proof that they accomplish the specified task. The third, and most important, is an experimental program which motivates and corrects or verifies the formalism. At the present time, robotics research in each of these categories flourishes only for purely geometric task domains such as navigation among fixed or moving obstacles. Task domains involving geometry and static forces such as peg insertion and other compliant tasks claim a growing share of attention. However work in any aspect of fully dynamical task domains is relatively rare.

Our paper focuses on the first and second aspect of this important but under-represented area of robotics, building on the significant contributions that Raibert and his colleagues have made in the second and third. That is, we attempt to account in some measure for the experimental success of Raibert's control strategies by adopting a formal representation of the task domain. Such a project, of course, is guaranteed to encounter the inevitable conflict between physical accuracy and analytical tractability, and it is just this tension which the paper explores. Apart from its academic interest — perspective in "hindsight" — this effort to understand the operating principles of an existing robot informs independent work that we are pursuing in the analysis and control of a throwing, catching, and juggling robot [1,4]. Our ultimate goal lies in a unified body of theory for robotics in intermittent dynamical environments which explains and is supported by representative experiments.

Specifically, this paper presents an initial exploration of certain analytical techniques from the theory of nonlinear discrete dynamical systems applied to the robotic domain of interest. The analysis relies upon exact integration of each "piece" of the robot-environment dynamical interaction. From these pieces we build a discrete "return" map for points on a fixed "section" in the phase space of the underlying continuous-time dynamics. Most relevant features of the qualitative behavior of the continuous system may be captured by the analysis of the resulting (one dimension smaller) discrete dynamics. In particular, we concentrate upon the global stability of a unique periodic orbit — a formalization of our intuitive sense of what would constitute

a successful hopping strategy.

In Section 2 we present a class of greatly simplified models of the robot in its environment based as closely as possible upon the insights and discussion in [5]. The models are simulated and compared in relation to physical experiments (as reported in [5]), to each other, and to the analytical results of Sections 3 and 4, which constitute the chief contribution of the paper. The highlights of this analysis are summarized in Theorem 1 of Section 3.2 and Theorem 2 of Section 4. The former states that a linear-spring based hopper, when subjected to a simplified version of the Raibert control scheme in a fairly accurate version of the true environment, is guaranteed to have a globally attracting stable periodic limiting trajectory. The latter states that an inverse-law-spring based hopper, when subjected to a closer approximation of the true Raibert control scheme in a trivialized version of the environment, will always have a periodic trajectory, but that this may be unstable, and, if it is, must evince a "doubly looped" trajectory in phase space — a "limping gate"[1] — whose stability properties remain to be established.

We are certainly encouraged by the degree to which these models admit a tractable analysis, while maintaining a reasonable resemblance to the physical phenomena which they purport to capture. While a variety of more sophisticated analytical issues suggest themselves, we are inclined toward circumspection about their relevance in the absence of more careful validation with respect to the physical apparatus.

[1]This phrase was coined by Raibert in a personal conversation.

2 Modeling and Simulations

In this Section, we construct a greatly simplified model of the hopper dynamics given in equation (4) based upon the discussion in Raibert's book [5]. Not surprisingly, it turns out that different simplifying assumptions concerning the hopper's actuators have significant implications for subsequent analytical tractability. In the second part of this Section we highlight the theoretical results whose formal proof constitutes the heart of the paper. In the last part of this Section, we illustrate the meaning of these results by presenting a variety of simulations of the model in contrast to the empirical data reported by Raibert.

2.1 A Model for a Vertically Hopping Robot

In the sequel we shall attempt to denote scalar quantities by greek letters, and vector quantities by roman letters. For example,

$$x \triangleq \begin{bmatrix} \chi \\ \dot{\chi} \end{bmatrix}$$

will denote the "state" of a one degree of freedom mass position, χ, and velocity, $\dot{\chi}$, with respect to the "x coordinate system".

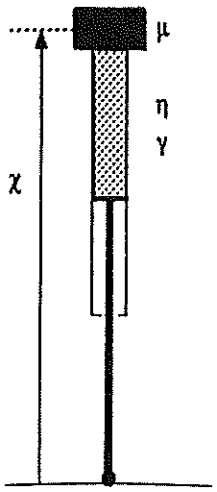

Figure 1: The simplified hopper model

Our abstraction of the vertical hopper consists of a body of unit mass ($\mu = 1$) and a leg of zero mass subject to viscous friction, γ, as depicted in Figure 1. The leg is "actuated" by some kind of energy storage mechanism, a device which exerts force in relation to position, $\varphi(\chi)$. The actuator is "controlled" by an adjustable "spring-constant" $\eta(\chi, \dot{\chi}, t)$ which multiplies the spring law, φ. We will find it useful to make a conceptual distinction between the "robot" — the nature of the spring mechanism, φ, and its feedback control strategy, η — and the "environment" — the friction in the leg, the force of gravity, the location of ground, etc.

In Raibert's hopper, the energy storage element is a pneumatic cylinder. Boyle's law states that the pressure of a fixed mass of an (ideal) gas is inversely proportional to its volume. Thus the pneumatic cylinder gives rise to the nonlinear inverse-law spring,

$$\varphi_{nl}(\chi) = 1/\chi.$$

To gain further analytical insight we will consider a linear spring law, φ_l, as well. Control input is implemented by connecting the cylinder to a constant supply pressure, and then turning the valves open or closed as a function of state feedback and time.

Specifically, Raibert divides the time of one complete vertical hop into four phases: compression, thrust, decompression and flight phase. The first three phases where the foot touches the ground are also called stance phase. At touchdown (t_{td}, x_{td}), an initial pressure exists in the leg, fixing the spring constant during compression, η_1. Starting at bottom (t_b, x_b), a condition defined by $\dot{\chi}_b(t_b) = 0$, the control valves are opened, the constant supply pressure is connected to the leg cylinder for a fixed time δ_t — "the thrust phase" — resulting in a constant force τ, the product of the supply pressure and the cross section of the pneumatic cylinder. In equations (1) and (2), this will be modeled as a continuous adjustment of the spring constant, which we denote η, such that the product $\eta\varphi$ yields the constant force τ over the entire course of the thrust phase. At the end of the thrust phase, (t_{et}, x_{et}), the valves are closed once again, *defining a new effective spring constant, η_2, for the duration of the subsequent decompression phase* . The new spring law constant, η_2 is, necessarily, a function of the body position at the end of the thrust-phase χ_{et}. The decompression phase occurs after thrust phase until liftoff, (t_l, x_l). Finally, the flight phase is the time from liftoff until the next touchdown. In this phase, the leg has no contact with ground, friction is zero and gravity is the only force present. Throughout this paper we make the assumption that liftoff and touchdown occurs at the same hight,

$$\chi_{td} = \chi_l > \chi_b$$

and for the linear spring $\chi_l = \chi_{td} = 0$ and $\chi_b < 0$ as well. In the latter case the position of the body with the spring relaxed is denoted by χ_0.

To summarize, for the nonlinear robot, φ_{nl}, the effective feedback control law may be specified as

$$\eta_{nl}(\chi, \dot{\chi}, t) = \begin{cases} \eta_1 & \text{if } \dot{\chi} < 0, \chi < \chi_{td} & \text{compression} \\ \tau\chi & \text{if } t \in (t_b, t_{et}) & \text{thrust} \\ \eta_2 = \tau\chi_{et} & \text{if } \dot{\chi} > 0, \chi_{et} < \chi < \chi_l & \text{decompression} \\ 0 & \text{otherwise} & \text{flight,} \end{cases} \tag{1}$$

and this would be analogous, in the case of a linear robot, φ_l, to the feedback law,

$$\eta_l(\chi, \dot{\chi}, t) = \begin{cases} \eta_1 & \text{if } \dot{\chi} < 0, \chi < \chi_{td} & \text{compression} \\ \frac{\tau}{\chi_0 - \chi} & \text{if } t \in (t_b, t_{et}) & \text{thrust} \\ \eta_2 = \frac{\tau}{\chi_0 - \chi_{et}} & \text{if } \dot{\chi} > 0, \chi_{et} < \chi < \chi_l & \text{decompression} \\ 0 & \text{otherwise} & \text{flight.} \end{cases} \tag{2}$$

The forces exerted by the robot upon the environment may now be written as

$$F_r \triangleq \ddot{\chi} - \eta(\chi, \dot{\chi}, t) \cdot \varphi(\chi).$$

At the same time, the environment interacts with the robot in response to the position and velocity of the latter. Namely, during the stance phase, viscous friction applies an opposing force to the motion of the leg, which disappears during flight. The gravitational constant, g, opposes upward motion everywhere. The forces exerted by the environment upon the robot might now be represented by the "strategy",

$$F_e \triangleq -g - \sigma(\chi)\gamma\dot{\chi},$$

where

$$\sigma(\chi) = \begin{cases} 1 & \text{if } \chi < \chi_l = \chi_{td} \quad \text{stance} \\ 0 & \text{otherwise} \qquad\quad \text{flight.} \end{cases} \tag{3}$$

Coupling the dynamical structure of the environment to the robot, $F_r = F_e$, now gives our model,

$$\ddot{\chi} + \sigma(\chi)\gamma\dot{\chi} - \eta(\chi, \dot{\chi}, t)\varphi(\chi) + g = 0. \tag{4}$$

2.2 Preview of Formal Results

First, we offer the result of an analysis of the linear spring version of (4) in the complete environment, F_e. We examine a "simplified" version of the control law, η_l, where the spring constant is unchanged before and after the thrust phase, and the touchdown and liftoff points lie on the same axis. This simplification affords rather strong analytical results. We will show that the "return map" for an energy-like quantity in the phase plane may be represented as:

$$\varphi_{j+1} = \left(\varphi_j + K_T^2\right) e^{-\pi K_D} \exp\left\{ K_D \arctan\left(\frac{K_T}{\sqrt{\varphi_j}}\right)\right\}, \tag{5}$$

where K_T is a parameter measuring the thrust at each bounce, and K_D essentially measures the damping ratio of a spring-mass-damper system. Moreover, we assert the following strong conclusion about the limiting behavior of this system.

Theorem 1 *The dynamical system 5 has a unique, globally attracting fixed point on the domain* $\mathcal{D} \triangleq (0, \infty)$.

This states that the linear spring based hopper, when subjected to a simplified version of the Raibert control scheme in a fairly accurate version of the true environment, is guaranteed to have a globally attractive stable periodic limiting trajectory.

Of course, in general, nonlinear differential equations resulting from the inverse spring law do not admit closed form integration, and we are forced to strip away a number of crucial aspects of the full nonlinear model in order to achieve an integrable system. Specifically, we remove the viscous friction forces and gravity during the stance phase and let the time of thrust go to zero. Again, assume that touchdown and liftoff points lie on the same axis. Similarly to the linear case, we obtain a discrete map between successive bottom points,

$$\chi_{j+1} = \chi_l \left(\frac{\chi_l}{\chi_j}\right)^{-\frac{\chi_j}{\chi^*}}. \tag{6}$$

Here the constant $\chi^* = \eta_1/\tau$, the quotient of the fixed spring constant during compression and the constant force during thrust phase, is the unique fixed point of this discrete map.

Theorem 2 *The system (6) has a unique fixed point on the domain* $\mathcal{D} \triangleq (0, \chi_l)$, *which is locally asymptotically stable if and only if* $\chi^* \in \mathcal{D}_1 \triangleq (\chi_l/e^2, \chi_l)$. *If* χ^* *is not a local attractor, i.e.,* $\chi^* \in (0, \chi_l/e^2) \triangleq \mathcal{D}_0$, *then there exists at least one orbit of period two, i.e. a fixed point of* $g \triangleq f \circ f$, *which is not a fixed point of* f.

The latter states that an inverse-law-spring based hopper, when subjected to a closer approximation of the true Raibert control scheme in a trivialized version of the environment, will always have a periodic trajectory, but that this may be unstable, and, if it is, must evince a "doubly looped" trajectory in phase space (i.e. there must be a period-two orbit of the discrete dynamical system), whose stability properties remain to be established.

2.3 Simulations

This section is intended as a rough validation of the simplifying assumptions about the hopping robot built into these models. We seek to suggest that their relevance to the physical phenomena and to each other is sufficiently great to motivate their subsequent analysis in Sections 3 and 4, below.

As a first cut check on the validity of our general model, we compare the various simulations with a plot of the physical system lifted straight out of Raibert's book — Figure 2. Starting at top, the vertical hopper goes through touchdown (note the counterclockwise direction) and compression to bottom. Some part of the trajectory until liftoff constitutes the thrust phase, which is not clearly distinguishable in this plot. After liftoff, the hopper completes the cycle at the top. The same sequence of events attaches to our simulation plots — Figures 3 through 10 — with the exception that they evolve in a clockwise fashion. Our figures depict, as well, transient trajectories: dashed trajectory leaves from initial conditions outside the closed curve and a solid line trajectory leaves from inside at the solid dot.

In Section 3, two versions of the linear robot model will be examined, and the environment model left intact. First, in Section 3.2, we consider the "simplified" case wherein the new spring constant during decompression is identical to that during the compression portion of the stance phase. Next, Section 3.3, considers the "complete" linear robot model as specified in equation (2). Figure 3 depicts a few typical trajectories of this model. For these parameter settings, reported in Table 1, the model bears striking resemblance to the experimental data shown in Figure 2. Perturbing the parameter settings does not greatly affect this resemblance. Next, consider Figures 4 and 5 — a depiction of trajectories from the simplified linear system with two sets of parameters as given in Table 1. While the transition between thrust and decompression phase seems exaggerated here relative to the earlier figures, the resemblance is still clear. To get some qualitative feeling for the undesirable artifacts introduced by the simplified linear model, the reader should note that our setting for gravity departs from reality in the simulation plotted in Figure 4, while the simulation plotted in Figure 5 has closer parameter values to those of Figure 3 yet presents a more distorted phase portrait.

Figure 7 depicts some sample trajectories of the complete robot-environment pair. There are some differences with the experimental data, Figure 2. In particular, these trajectories do not have the same symmetry. However, qualitatively, the plots seem to correspond for reasonable initial conditions, even under reasonable parametric perturbations. The word reasonable deserves some further attention here. For sufficiently large initial velocities, the simulated ball may impact with such great kinetic energy that the reaction spring force potential at the bottom point exceeds the simulated fixed supply pressure feeding the valves. We presume that this "potential energy dissipation regime", while not always easy to avoid in simulation, is most likely an artifact, and would not occur in a physical experiment.

Section 4 presents a formal treatment of the nonlinear problem. Here, the attempt at analytical tractability suggests significant changes in both the robot and environment models. In particular, we reduce the thrust interval to zero in the robot model while still maintaining the effective change of spring constant and thus of the total system energy at the bottom . We alter the environment by removing the force of gravity during stance. A still greater departure from the real environment is the removal of the viscous friction term during stance as well. This evidently implies that all energy dissipation occurs in the presumably spurious potential-dissipation regime. Nevertheless, a glance at Figure 6 shows that it is not terribly unlike any of the other plots.

We may now consider the relationship of the simulations to the formal results of the following two sections. There, the chief concern is to find conditions under which the robot will "settle down" to a periodic trajectory. In the terms of the formalism, this corresponds to a "stable attracting fixed point" of the derived discrete map. The simulations of the simplified linear robot model, Figure 4 and the simplified nonlinear model, Figure 6, reflect the fact that both systems have unique attracting fixed points, conditions for which are given, respectively, by Theorem 1 and Theorem 2. Again, the trajectories of the simplified nonlinear model, Figure 6, and of the complete nonlinear model, Figure 7, exhibit surprising resemblance. In particular, both show trajectory crossing, and the characteristic "double loop" trajectories — a period two orbit of the discrete dynamical system predicted by Proposition 4.3 . For the simple nonlinear system, Figure 10 depicts unstable motion around the period one orbit and at the same time, we can see in Figure 8 a period two orbit of the same system.

2.4 Simulation Figures and Parameter Table

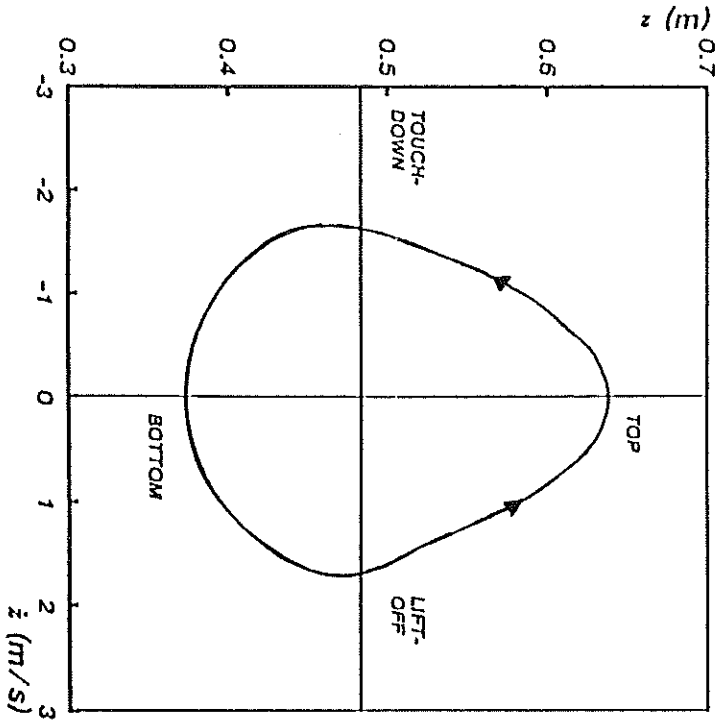

Figure 2: Raibert's Hopper

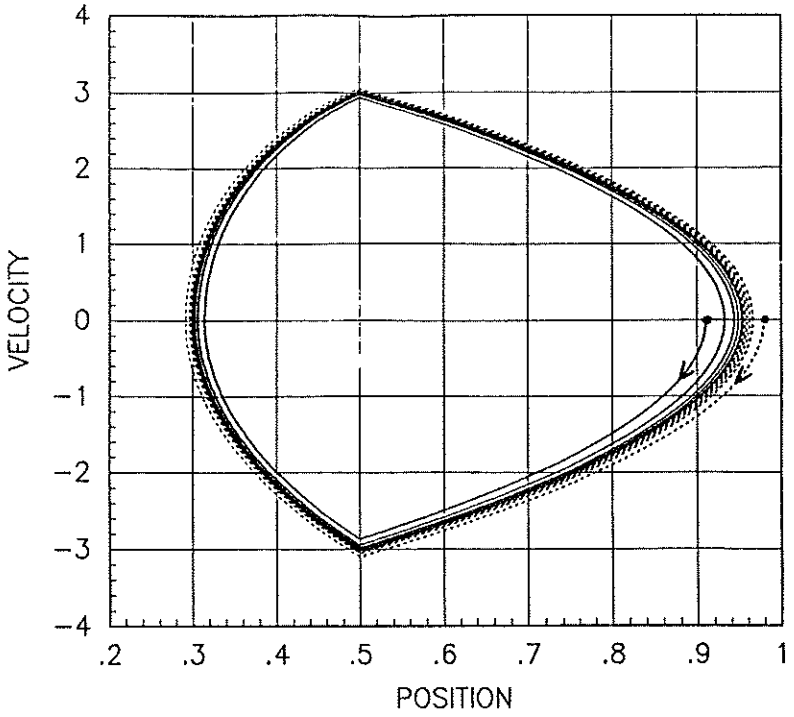

Figure 3: The complete linear Hopper (Section 3.3, Equations (2) and (4))

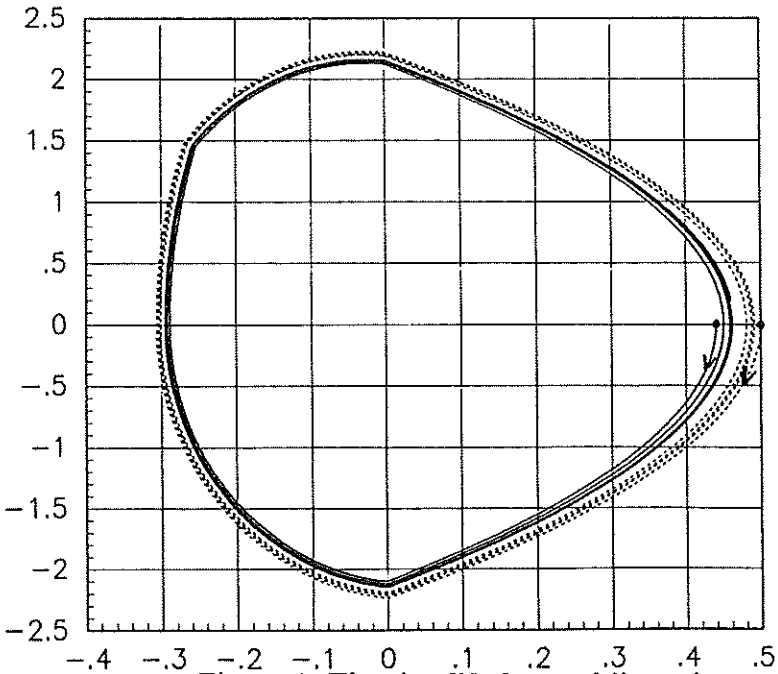

Figure 4: The simplified, tuned linear hopper (Section 3.2)

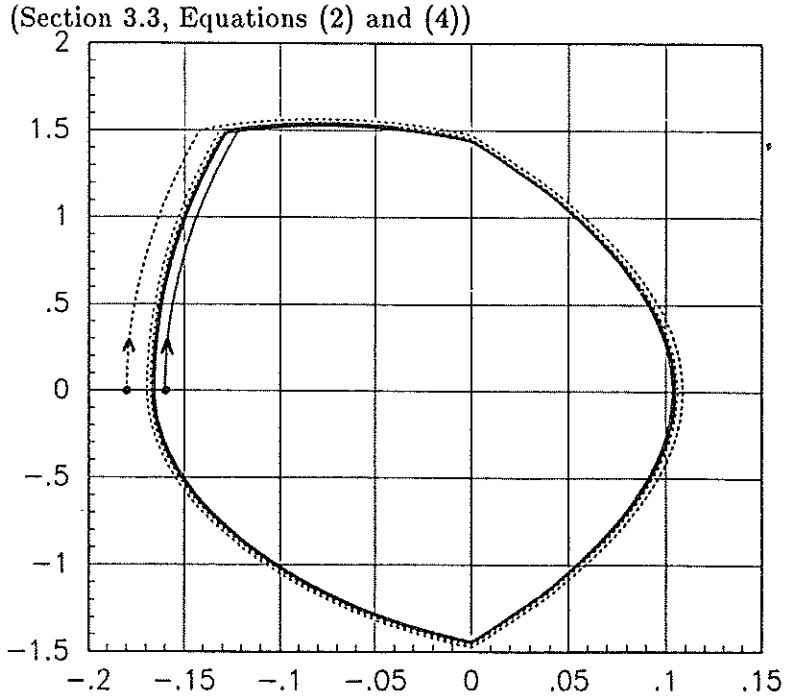

Figure 5: The simplified linear hopper (Section 3.2)

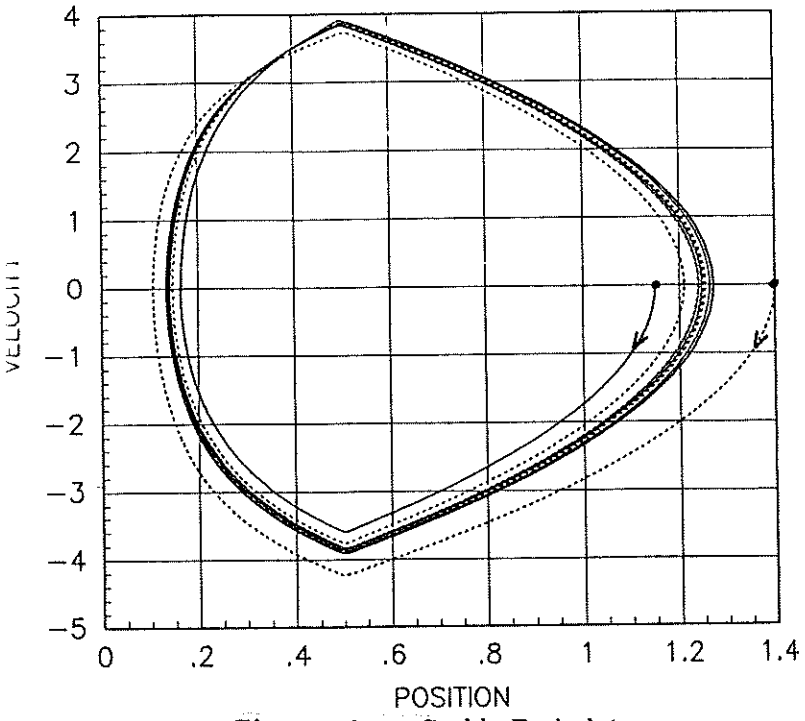

Figure 6: Stable Period 1, nonlinear simplified hopper (Section 4.2, Proposition 4.2)

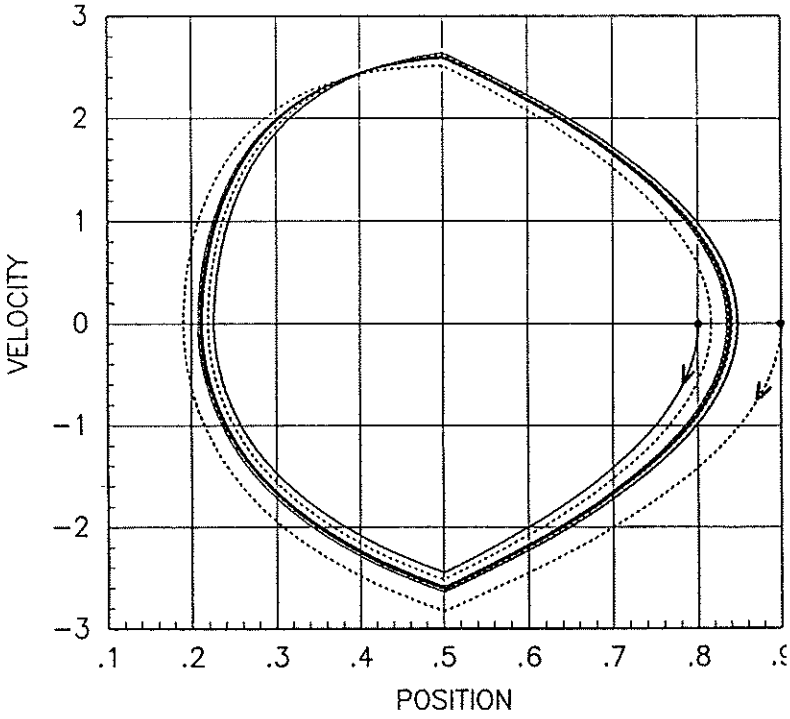

Figure 7: Stable Period 1, nonlinear complete hopper (Equations (1) and (4))

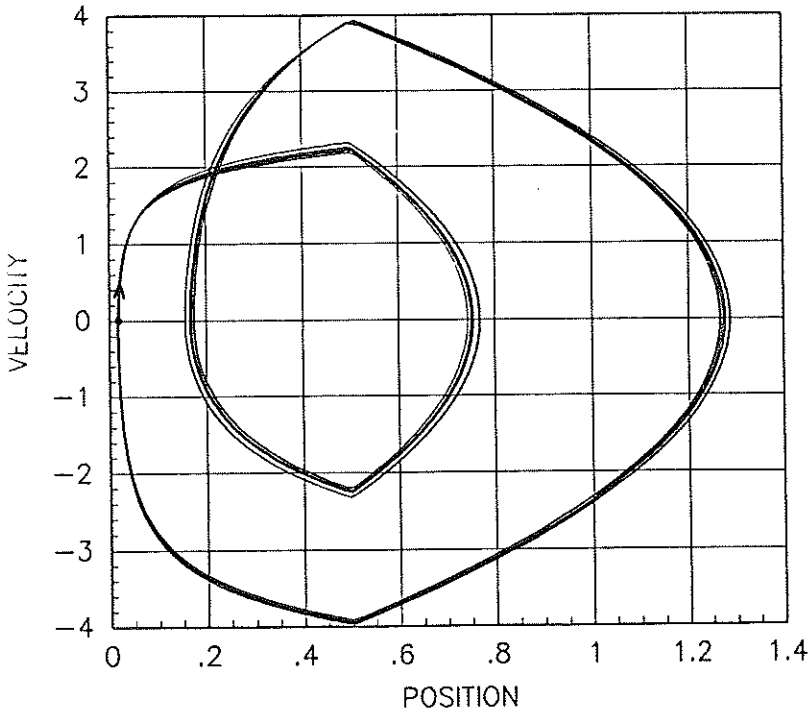

Figure 8: Stable Period 2, nonlinear simplified hopper (Proposition 4.3)

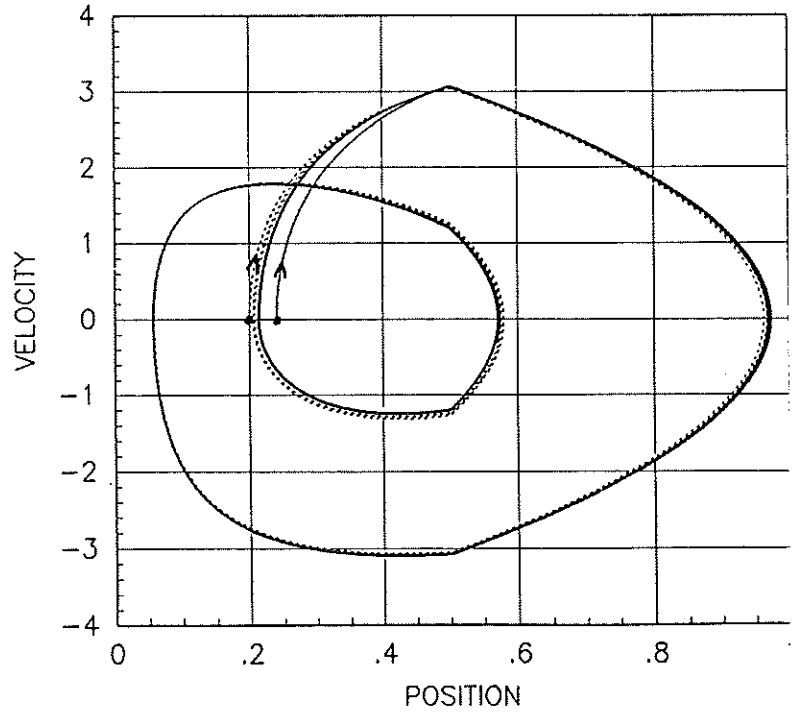

Figure 9: Stable Period 2, nonlinear complete hopper (Equations (1) and (4))

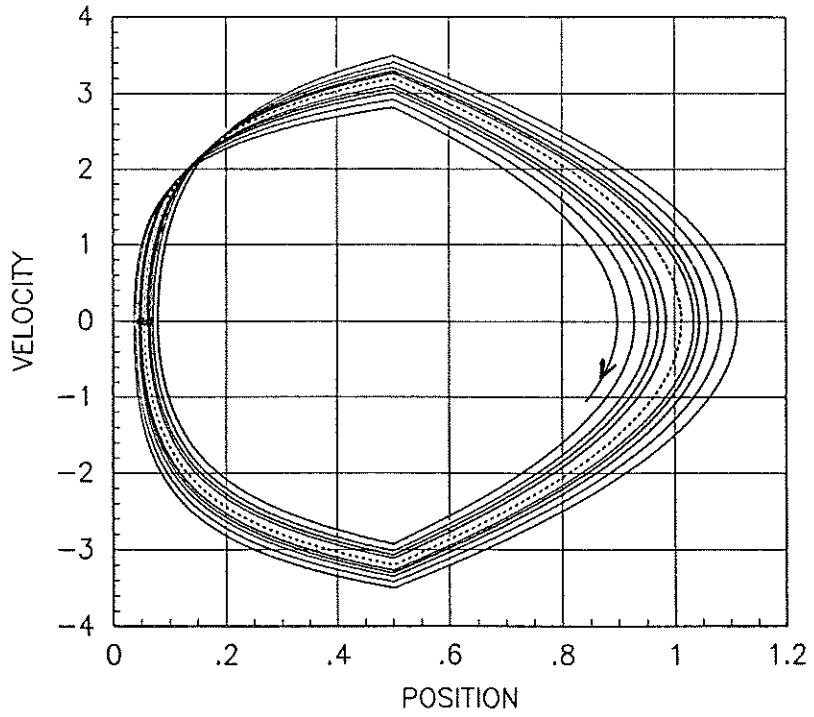

Figure 10: Unstable Period 1, nonlinear simplified hopper (Proposition 4.2)

Figure	Initial Position		Liftoff Pos.	Thrust Time	Thrust Force	Friction Constant	Initial Spring Const.	Gravit. Const.	Spring Relax. Position
	$\chi(0)$		χ_l	δ_l	τ	γ	η_1	g	χ_0
3	0.91	0.98	0.5	0.05	41.86	2.33	46.5	10	1
4	0.44	0.5	0	0.05	41.86	0.58	46.5	5	0.1
5	-0.16	-0.18	0	0.05	41.86	2.33	46.5	10	0.215
6	0.12	0.14	0.5	0	41.86	0	5.81	0/10	N/A
7	0.8	0.9	0.5	0.01	41.86	2.33	5.81	10	N/A
8	0.02		0.5	0	41.86	0	2.33	0/10	N/A
9	0.2	0.24	0.5	0	41.86	0.06	4.186	10	N/A
10	0.056	0.06	0.5	0	41.86	0	2.33	0/10	N/A

Table 1: Simulation Parameters

3 Analysis of a Linear Model

This section offers an analysis of the linear spring version of (4) in the complete environment, F_e, as defined in Section 2.1. We proceed by building a return map for iterates of an energy-like quantity in the phase plane. This "normalized" energy is defined and its desirable properties are presented in Section 3.1. We examine in Section 3.2 a "simplified" version of the control law, η, in some detail, for this simplification affords rather strong analytical results. Namely, we present a complete analysis of all possible periodic trajectories, as summarized in Theorem 1. Finally, in Section 3.3, we consider the full linear robot model, F_r, as defined in Section 2.1. We show that there is no fundamental difference in the two cases by building a return map for the same quantity using nearly identical methods. However, the the resulting discrete dynamical system is considerably messier, and its qualitative properties remain to be established.

3.1 Normalized Energy for Translated Focal Linear Systems

Consider the autonomous planar dynamics,

$$\dot{x} = Ax + b, \tag{7}$$

a linear system forced by a constant disturbance input. In the "focal" case where $A \in \mathbb{R}^{2\times 2}$ has complex conjugate eigenvalues (we will assume they have negative real part),

$$spectrum(A) = \{-\sigma + i\omega,\ -\sigma - i\omega\},$$

there is a new coordinate system achieved by a translation and change of basis,

$$y \triangleq W(x + A^{-1}b),$$

with respect to which the dynamical system is linear,

$$\dot{y} = \bar{A}y,$$

and

$$\bar{A} = WAW^{-1} = -\sigma I + \omega J.$$

constitutes the "normalized form" of A. Here, I is the identity matrix and $J = -J^{\mathrm{T}}$ is the unit skew symmetric matrix of $\mathbb{R}^{2\times 2}$,

$$J \triangleq \begin{bmatrix} 0 & 1 \\ -1 & 0 \end{bmatrix}.$$

In the new system, we may define the "normalized energy" to be

$$\vartheta \triangleq y^{\mathrm{T}}y,$$

and the "normalized angle" to be

$$\theta \triangleq \arctan[y_2/y_1],$$

yielding the normal polar coordinate system system

$$\begin{aligned} \dot{\vartheta} &= -2\sigma\vartheta \\ \dot{\theta} &= \omega \end{aligned}$$

whose solutions may be parametrized by θ as

$$\vartheta(\theta) = \vartheta(\theta_0)\exp\left\{2\frac{-\sigma}{\omega}[\theta-\theta_0]\right\}. \tag{8}$$

In particular, suppose A is specified in phase canonical form,

$$\begin{aligned} A &= \begin{bmatrix} 0 & 1 \\ -\kappa & -\gamma \end{bmatrix} \\ &= \begin{bmatrix} -\frac{1}{2}\gamma & 0 \\ 0 & -\frac{1}{2}\gamma \end{bmatrix} + \begin{bmatrix} 0 & 1 \\ -1 & 0 \end{bmatrix}\begin{bmatrix} \kappa & \frac{1}{2}\gamma \\ \frac{1}{2}\gamma & 1 \end{bmatrix} \\ &= -\tfrac{1}{2}\gamma I + JP. \end{aligned} \tag{9}$$

The system is focal if $\gamma^2 < 4\kappa$ in which case P has a real "square root"

$$P = W^{\mathrm{T}}W,$$

given by

$$W \triangleq \frac{1}{\sqrt{\kappa}}\begin{bmatrix} \kappa & \frac{1}{2}\gamma \\ 0 & \sqrt{\kappa-\gamma^2/4} \end{bmatrix}.$$

Now, if $y = Wx$, it follows that

$$\dot{y} = WAx = \left[-\frac{1}{2}\gamma I + WJW^{\mathrm{T}}\right]y$$

is, indeed, the normalized system, since

$$WJW^{\mathrm{T}} = J\sqrt{\kappa-\gamma^2/4}.$$

We have, then,

$$\sigma \triangleq \frac{1}{2}\gamma; \qquad \omega \triangleq \sqrt{\kappa-\gamma^2/4}.$$

Note that while the traditional "mechanical energy" — the total kinetic plus potential energy — of this system is given by

$$\vartheta_E(x) \triangleq x^{\mathrm{T}}\begin{bmatrix} \kappa & 0 \\ 0 & 1 \end{bmatrix}x,$$

our "normalized" energy is expressed as

$$\vartheta(x) \triangleq \left[x + A^{-1}b\right]^{\mathrm{T}}\begin{bmatrix} \kappa & \frac{1}{2}\gamma \\ \frac{1}{2}\gamma & 1 \end{bmatrix}\left[x + A^{-1}b\right]$$

in the disturbed phase canonical coordinate system.

3.2 Vertical Hopper with Fixed Linear Spring

Now consider the following simplification of the linear version of system 4. Assume that the spring constant is unchanged before and after the thrust phase,

$$\eta_1 = \eta_2 = \kappa, \tag{10}$$

and that it has been chosen, along with the relaxation position, χ_0, to place the zero potential energy position exactly on the ordinate of the original coordinate system,

$$\kappa = g/\chi_0. \tag{11}$$

Moreover, due to energy conservation during flight, $\dot{\chi}_{td} = -\dot{\chi}_l$, such that

$$x_{td} = -x_l = \begin{bmatrix} 0 \\ -\dot{\chi}_l \end{bmatrix}.$$

The resulting vector field during stance is given by equation (7) with the entries of A as specified in (9) and disturbance given by

$$b = \begin{bmatrix} 0 \\ \kappa\chi_0 - g \end{bmatrix} = 0.$$

During the flight phase, the hopper experiences a constant acceleration due to gravity, g, and during the thrust phase, both a constant force, τ, as well as a force proportional to velocity due to friction, γ.

At time t_b, the bottom of the stance phase, suppose the hopping ball is at state

$$x_b \triangleq \begin{bmatrix} -\chi_b \\ 0 \end{bmatrix}.$$

It follows that the normalized energy at this point is

$$\vartheta_b \triangleq \vartheta(x_b) = x_b^{\mathrm{T}} P x_b = \kappa\chi_b^2 = \psi_b^2.$$

According to our model, the hopper next experiences a fixed thrust and viscous damping over the period of time, $\delta_l \triangleq t_{el} - t_b$ with the result that

$$x_{el} = x_b + x_l,$$

where

$$x_l = \begin{bmatrix} \chi_l \\ \dot{\chi}_l \end{bmatrix} = \begin{bmatrix} \tau[\gamma\delta_l - 1 + e^{-\gamma\delta_l}]/\gamma^2 \\ \tau[1 - e^{-\gamma\delta_l}]/\gamma \end{bmatrix},$$

hence,

$$y_l = \begin{bmatrix} \psi_l \\ \dot{\psi}_l \end{bmatrix} = W x_l.$$

It follows that

$$\begin{aligned}\vartheta_{et} &\triangleq \vartheta(x_b + x_t)\\ &= [\psi_t - \psi_b]^2 + \dot{\psi}_t^2\\ &= [\psi_t - \sqrt{\vartheta_b}]^2 + \dot{\psi}_t^2.\end{aligned}$$

The trajectory during decompression between t_{et} and t_l is governed by the linear system solved in equation (8) with the result that

$$\vartheta_l \triangleq \vartheta(x_l) = \vartheta_{et} \exp\left\{-\frac{2\sigma}{\omega}[\theta_{et} - \theta_l]\right\},$$

where, under the assumption that $\chi_b > \chi_t$,

$$\theta_{et} \triangleq \pi - \arctan\left(\frac{\dot{\psi}_t}{\sqrt{\vartheta_b} - \psi_t}\right), \qquad \theta_l \triangleq \arctan\left(\frac{y_2(t_l)}{y_1(t_l)}\right).$$

Note, importantly, that since we have assumed zero disturbance, $b = 0$, and liftoff on the ordinate,

$$x_l = \begin{bmatrix} 0 \\ \dot{\chi}_l \end{bmatrix},$$

the ratio,

$$\frac{y_2(t_l)}{y_1(t_l)} = \frac{\sqrt{4\kappa - \gamma^2}}{\gamma}$$

is independent of $\dot{\chi}_l$, and θ_l is identical for each cycle.

In flight, the hopper is subjected to a constant negative acceleration due to gravity, and we may suppose that $x_{td} = -x_l$, hence, $y_{td} = -y_l$, and $v_{td} = v_l$. Between t_{td}, and t_b, the energy evolves, again, according to (8), with the result that at the next bottom we have

$$\begin{aligned}\vartheta_{b,next} = \; &= \vartheta_{td} \exp\left\{-\tfrac{2\sigma}{\omega}[\theta_{td} - \theta_b]\right\}\\ &= \vartheta_l \exp\left\{-\tfrac{2\sigma}{\omega}\theta_l\right\}\\ &= \vartheta_{et} \exp\left\{-\tfrac{2\sigma}{\omega}\theta_{et}\right\}\\ &= \left([\psi_t - \sqrt{\vartheta_b}]^2 + \dot{\psi}_t^2\right) \exp\left\{-\tfrac{2\sigma}{\omega}\left[\pi - \arctan\left(\tfrac{\dot{\psi}_t}{\sqrt{\vartheta_b} - \psi_t}\right)\right]\right\}\\ &\triangleq f(\vartheta_b).\end{aligned}$$

Thus, we obtain a first order discrete nonlinear dynamical system in the normalized energy at successive bottom points,

$$\vartheta_{j+1} = f(\vartheta_j). \tag{12}$$

According to the assumptions made in the course of the derivation, the iterates of this scalar system, $\{\vartheta_j\}_0^\infty$, starting from the initial conditions $\vartheta_0 \triangleq \vartheta[x_b(0)]$ describe exactly the future "bottom points" in phase space,

$$(x_b)_j = \begin{bmatrix} -\sqrt{\vartheta_j/\kappa} \\ 0 \end{bmatrix},$$

providing $\vartheta_j > \psi_l^2$.

We are now in a position to provide conditions on the parameters which guarantee that the hopper tends toward a stable periodic motion from all initial conditions. In the sequel, it will be useful to shift the origin of the discrete system 12, by defining

$$\varphi \triangleq \left[\sqrt{\vartheta} - \psi_l\right]^2,$$

and then viewing f as the product $f_1 f_2$ where

$$f_1(\varphi) \triangleq \varphi + \dot{\psi}_l^2$$

expresses the energy gained during the thrust phase, and

$$f_2(\varphi) \triangleq e^{-\frac{2\sigma\pi}{\omega}} \exp\left\{\frac{2\sigma}{\omega} \arctan\left(\frac{\dot{\psi}_l}{\sqrt{\varphi}}\right)\right\}$$

expresses the energy lost to friction during a single cycle. Note, once again, that the domain upon which this system is well defined may be written as

$$\mathcal{D} \triangleq (0, \infty)$$

in the translated φ-coordinate system.

Proposition 3.1 *The dynamical system 12 has a unique fixed point on the domain, $\mathcal{D}$, defined with respect to the φ-coordinate system.*

Proof: Define the "ratio map",

$$r(\varphi) \triangleq f(\varphi)/\varphi.$$

Since $f(\varphi) = \varphi$ if and only if $r(\varphi) = 1$, it suffices to show that r is strictly decreasing and attains values both greater than and less than unity on $\mathcal{D}$. For r is continuous on $\mathcal{D}$, and this would imply the existence of a unique unity crossing of r, which, in turn, implies a unique fixed point of f.

Letting $r_1 \triangleq f_1/\varphi$, so that $r = r_1 f_2$, we have

$$\lim_{\varphi\to\infty} r_1 = 1, \qquad \lim_{\varphi\to\infty} f_2 = e^{-\frac{2\sigma\pi}{\omega}},$$

and it is clear that r achieves values less than unity for sufficiently large values of its argument. Moreover,

$$\lim_{\varphi\to 0} r_1 = \infty, \qquad \lim_{\varphi\to 0} f_2 = e^{-\frac{\sigma\pi}{\omega}},$$

and r certainly achieves values greater than unity on $\mathcal{D}$ as well.

Finally, to see that r is monotone down, note that both r_1 and f_2 are strictly positive and both are monotone down on $\mathcal{D}$. Thus,

$$\frac{dr}{d\varphi} = \frac{dr_1}{d\varphi} f_2 + r_1 \frac{df_2}{d\varphi},$$

being the sum of two negative numbers is itself negative.

□

It turns out that the unique fixed point guaranteed by the previous result may be shown to be a local attractor, and, moreover, is globally attracting on the entire domain, $\mathcal{D}$. In order to show this we will make use of the following two facts about f.

Lemma 3.2 *The discrete map, $f(\varphi)$, is monotone increasing on the domain*

$$\mathcal{D}_1 \triangleq \left(\left[\frac{\sigma \dot{\psi}_t}{\omega} \right]^2, \infty \right),$$

and monotone increasing on its complement,

$$\mathcal{D}_0 \triangleq \mathbb{R}^+ - \mathcal{D}_1.$$

Proof: First note that

$$\begin{aligned} \frac{df_2}{d\varphi} &= -f_2 \cdot \frac{2\sigma\dot{\psi}_t}{\omega\left(\varphi+\dot{\psi}_t^2\right)} \cdot \frac{1}{2\sqrt{\varphi}} \\ &= -f_2 \cdot \frac{\sigma\dot{\psi}_t}{\omega\sqrt{\varphi}} / f_1 \\ &\triangleq -f_2 \cdot f_3 / f_1. \end{aligned}$$

But

$$\begin{aligned} \frac{df}{d\varphi} &= f_2 \frac{df_1}{d\varphi} - f_1 (f_2 \cdot f_3 / f_1) \\ &= f_2 [1 - f_3], \end{aligned}$$

hence $\frac{df}{d\varphi} > 0$ if and only if

$$\sqrt{\varphi} > \sigma\dot{\psi}_t / \omega,$$

as stated.

□

Lemma 3.3 *If the magnitude of the derivative of f is greater than unity,*

$$\left| \frac{df}{d\varphi} \right| > 1$$

then the ratio map must be greater than unity as well,

$$r(\varphi) > 1.$$

Proof: First note that if $\varphi \in \mathcal{D}_1$, then, following the proof of Lemma 3.2 , the derivative could never have a magnitude greater than unity since it is the product of two functions, f_2, and $|1 - f_3|$ whose magnitude is smaller than unity on that interval. Thus, it remains to prove the result on $\mathcal{D}_0$.

Assuming the contrary, i.e. if

$$\begin{aligned} 1 &< \left|\frac{df}{d\varphi}\right| \\ &= f_2 \left|1 - \dot{\psi}_l \sigma / \sqrt{\varphi}\omega\right| \\ &= r\frac{\varphi}{\varphi + \dot{\psi}_l^2} \cdot \left|1 - \dot{\psi}_l \sigma / \sqrt{\varphi}\omega\right|, \end{aligned}$$

while $r < 1$, then it must also be true that

$$1 < \frac{\left|\varphi - \sqrt{\varphi}\dot{\psi}_l \sigma / \omega\right|}{\varphi + \dot{\psi}_l^2}$$

on $\mathcal{D}_0$. But

$$sup_{\varphi \in \mathcal{D}_0} = \dot{\psi}_l^2 \sigma^2 / 4\omega^2$$

occurs at $\varphi_{max} = \dot{\psi}_l^2 \sigma^2 / 2\omega^2$, thus the last fraction can never be greater than unity, and the contrary assumption has been shown to generate a contradiction.

□

The reader who is familiar with the analysis of discrete dynamical systems will note that the previous result already assures us that the unique fixed point is locally asymptotically stable. The following more general argument lays the groundwork for the final demonstration in Theorem 1 that condition gives global results as well.

Proposition 3.4 *If the continuously differentiable scalar map, $f \in C^1[\mathbb{R}]$, has a unique fixed point, φ^*, on some interval, $\mathcal{D} \subset \mathbb{R}$, and admits the bound*

$$\left|\frac{df}{d\varphi}\right| < 1,$$

on $\mathcal{D}$, then φ^* is a stable attractor of the discrete dynamical system,

$$\varphi_{j+1} = f(\varphi_j), \tag{13}$$

whose domain of attraction includes $\mathcal{D}$.

Proof: We will show that

$$\lambda(\varphi) \triangleq [\varphi - \varphi^*]^2,$$

is a global Lyapunov function for system (13) at φ^* over the entire domain $\mathcal{D}$. Since λ is clearly positive definite at the fixed point, and radially unbounded on $\mathcal{D}$, it will suffice to show that the function has has a negative definite first difference along the iterates of system.

To see this is so, note

$$\begin{aligned}\lambda_{j+1}(\varphi) - \lambda_j(\varphi) &= [f(\varphi) - \varphi^*]^2 - [\varphi - \varphi^*]^2 \\ &= f^2 - \varphi^2 - 2\varphi^*(f - \varphi) \\ &= (f - \varphi)(f + \varphi - 2\varphi^*).\end{aligned}$$

Form the partition, $\mathcal{D} = \mathcal{D}_- \cup \mathcal{D}_+$ where $\mathcal{D}_-$ is the open interval to the left of φ^* and $\mathcal{D}_+$ is the open interval to the right. Now observe that the first term of this product is sign definite on $\mathcal{D} - \{\varphi^*\}$ or else there would be another fixed point on the interval. In particular, the term must be strictly positive on $\mathcal{D}_-$, and strictly negative on $\mathcal{D}_+$, or else the derivative bound would fail at φ^*. Thus the proof is complete if we can show that the second term has strictly opposing sign on those intervals.

Suppose, to the contrary, that $(f + \varphi - 2\varphi^*)$ is positive or zero at some point, $\varphi_0 \in \mathcal{D}_-$, i.e.

$$f(\varphi_0) = 2\varphi^* - \varphi_0 + \epsilon,$$

for some $\epsilon \geq 0$. Then, according to the mean value theorem, there must be some point, $\tilde{\varphi} \in (\varphi_0, \varphi^*)$ at which

$$\begin{aligned}\tfrac{df}{d\varphi}\,|_{\tilde{\varphi}} &= \tfrac{f(\varphi^*) - f(\tilde{\varphi})}{\varphi^* - \tilde{\varphi}} \\ &= \tfrac{\varphi^* - [2\varphi^* - \tilde{\varphi} + \epsilon]}{\varphi^* - \tilde{\varphi}} \\ &= \tfrac{\tilde{\varphi} - \varphi^* - \epsilon}{\varphi^* - \tilde{\varphi}} \\ &= -1 - \tfrac{\epsilon}{\varphi^* - \tilde{\varphi}},\end{aligned}$$

in violation of the hypothesized bound. A similar observation applies to the other interval.

□

These technical results, now afford a global picture of the hopper's limiting behavior, expressed as follows.

Theorem 1 *The dynamical system 12 has a unique, globally attracting fixed point on the domain $\mathcal{D}$.*

Proof: The unique fixed point guaranteed in Proposition 3.1 lies in a domain, $\mathcal{D}_b$, where, according to to Lemma 3.3 , the derivative of f is bounded in magnitude by unity. It follows, from Theorem 1, that the fixed point is asymptotically stable, and

includes $\mathcal{D}_b$ in its domain of attraction. We may conclude the proof by showing that f maps the remaining interval, $\mathcal{D}_u \triangleq \mathbb{R}^+ - \mathcal{D}_b$ into $\mathcal{D}_b$, and, hence, the entirety of $\mathcal{D}$ is attracted to its unique fixed point.

First note that f is monotone down on $\mathcal{D}_u$, according to Lemma 3.2 . Moreover, $f(\varphi) > \varphi$ on $\mathcal{D}_u$, since Lemma 3.3 guarantees that $r < 1$ only in $\mathcal{D}_b$. Now identify the the common boundary point of the two intervals as, $\varphi_c \in \overline{\mathcal{D}_u} \cap \overline{\mathcal{D}_b}$. We observe that if $\varphi \in \mathcal{D}_u$, or equivalently,

$$\varphi \leq \varphi_c,$$

then

$$\varphi_c < f(\varphi_c) < f(\varphi),$$

or, equivalently, $f(\varphi) \in \mathcal{D}_b$.

□

3.3 Vertical Hopper with Shifting Linear Spring Constants

We next consider the full linear version of system 4. Namely, the spring constant after touch down and before the bottom point is some quantity fixed in advance,

$$\eta_1 \triangleq \kappa,$$

while its value after thrust and before liftoff is a function of the thrust force, τ, and the position in the phase plane at time of end-thrust, χ_{et} given as

$$\eta_2(j) \triangleq \frac{\tau}{\chi_0 - \chi_{et}(j)}.$$

We assume again that the touchdown/liftoff points lie on the same axis. Similarly, we will still assume that the fixed spring constant and relaxation point have been adjusted to coincide with this axis, i.e.

$$\eta_1 = g/\chi_0,$$

and the normalizing coordinate transformation before thrust is the same,

$$y \triangleq W(x + A^{-1}b); \qquad b \triangleq 0; \qquad W \triangleq \frac{1}{\sqrt{\eta_1}} \begin{bmatrix} \eta_1 & \frac{1}{2}\gamma \\ 0 & \sqrt{\eta_1 - \gamma^2/4} \end{bmatrix}.$$

However, the since the effective spring constant after thrust changes with each cycle, we shall require a different coordinate transformation for each new second stance phase,

$$z \triangleq U(x + c); \quad c \triangleq A^{-1}b = \begin{bmatrix} g/\eta_2(j) - \chi_0 \\ 0 \end{bmatrix}; \quad U \triangleq \frac{1}{\sqrt{\eta_2(j)}} \begin{bmatrix} \eta_2(j) & \frac{1}{2}\gamma \\ 0 & \sqrt{\eta_2(j) - \gamma^2/4} \end{bmatrix}.$$

It will be convenient in the sequel to denote the normalized energy in the y-coordinate system as ϑ, and the corresponding quantity in the z-coordinate system as ϑ'. Similarly, the primed version of all other symbols defined in the y system will denote their z counterparts.

Following the derivation in the previous section, suppose

$$x_b = \begin{bmatrix} -\chi_b \\ 0 \end{bmatrix}$$

at time t_b, so that $\vartheta_b = \eta_1 \chi_b^2$,

$$x_{et} = x_b + x_t,$$

as before, and

$$\vartheta_{et} = (\psi_t - \sqrt{\vartheta_b})^2 + \dot{\psi}_t^2.$$

The analysis must now depart from the earlier example, since the simple solution (8) during decompression relies upon the shifting z coordinates.

We first form the expression for ϑ'_{et} as a function of ϑ_b. This obtains from

$$\begin{aligned}
\vartheta'_{et} &= [x_{et} + c]^{\mathrm{T}} P' [x_{et} + c]^{\mathrm{T}} \\
&= [\tilde{\gamma}(\tilde{\chi}_t - \chi_b),\ \dot{\chi}_t] \begin{bmatrix} \eta_2 & \gamma/2 \\ \gamma/2 & 1 \end{bmatrix} \begin{bmatrix} \tilde{\gamma}(\tilde{\chi}_t - \chi_b) \\ \dot{\chi}_t \end{bmatrix} \\
&= [\tilde{\gamma}(\tilde{\chi}_t - \chi_b),\ \dot{\chi}_t] \begin{bmatrix} -\tau/(\tilde{\chi}_t - \chi_b) & \gamma/2 \\ \gamma/2 & 1 \end{bmatrix} \begin{bmatrix} \tilde{\gamma}(\tilde{\chi}_t - \chi_b) \\ \dot{\chi}_t \end{bmatrix} \\
&= \bar{\gamma}(\tilde{\chi}_t - \chi_b) + \dot{\chi}_t^2 \\
&= \bar{\gamma}\tilde{\chi}_t - (\bar{\gamma}/\sqrt{\eta_1})\sqrt{\vartheta_b} + \dot{\chi}_t^2 \\
&\triangleq \xi_1(\vartheta_b),
\end{aligned}$$

where

$$\begin{aligned}
\bar{\gamma} &\triangleq \tilde{\gamma}(\gamma\dot{\chi}_t - \tilde{\gamma}\tau) \\
\tilde{\gamma} &\triangleq 1 - g/\tau \\
\tilde{\chi}_t &\triangleq \chi_t - \chi_0.
\end{aligned}$$

Since the liftoff state,

$$z_t = U[x_t + c],$$

lies on an affine line instead of a line through the origin in the z coordinate system, θ'_t, the angle of liftoff in the z coordinate system is not a constant over each cycle, and the analysis is simplified by parametrizing ϑ' according to time,

$$\vartheta'_t = \vartheta'_{et} \exp\{-2\sigma(t_t - t_{et})\}.$$

For the time elapsed during decompression is, of course, the same in the y and z coordinate systems, and, in the y system, $\frac{d\theta}{dt} = \omega$ implies

$$t_t - t_{et} = \frac{1}{\omega}\left[\pi - \arctan\left(\frac{\dot{\psi}_t}{\sqrt{\vartheta_b} - \psi_t}\right) - \arctan\left(\frac{y_2(t_t)}{y_1(t_t)}\right)\right],$$

as in the previous section. Thus, we have

$$\begin{aligned}\vartheta_l' &= \xi_1(\vartheta_b)\exp\left\{\left[\pi - \arctan\left(\frac{\dot\psi_l}{\sqrt{\vartheta_b}-\psi_l}\right) - \arctan\left(\frac{y_2(t_l)}{y_1(t_l)}\right)\right],\right\}\\ &\triangleq \xi_2(\vartheta_b).\end{aligned}$$

After liftoff, we must express the normalized energy of the z coordinate system, ϑ_l', as a normalized energy in the y system. This may be readily accomplished as follows. Note that

$$\vartheta_l = x_l^{\mathrm{T}} P x_l = \dot\chi_l^2.$$

Moreover,

$$\begin{aligned}\vartheta_l' &= [x_l + c]^{\mathrm{T}} P' [x_{el} + c]^{\mathrm{T}}\\ &= [(g/\tau)(\tilde\chi_l - \chi_b) - \chi_0,\ \dot\chi_l]\begin{bmatrix} -\tau/(\tilde\chi_l - \chi_b) & \gamma/2 \\ \gamma/2 & 1\end{bmatrix}\begin{bmatrix}(g/2)(\tilde\chi_l - \chi_b) - \chi_0 \\ \dot\chi_l\end{bmatrix}\\ &= \gamma\tilde\chi_l - \gamma'\chi_b + \dot\chi_l^2 - \chi_0(\dot\chi_l - 2g) - \frac{\chi_0^2\tau}{\tilde\chi_l - \chi_b}\\ &= \gamma\tilde\chi_l - (\gamma'/\sqrt{\eta_1})\sqrt{\vartheta_b} + \vartheta_l - \chi_0(\sqrt{\vartheta_l} - 2g) - \frac{\chi_0^2\tau}{\tilde\chi_l - (1/\sqrt{\eta_1})\sqrt{\vartheta_b}},\end{aligned}$$

where

$$\gamma' \triangleq (g/\tau)(\gamma\dot\chi_l - g),$$

and the other symbols are defined above. Thus, ϑ_l is related to ϑ_l' and ϑ_b as

$$\begin{aligned}\vartheta_l - \chi_0\sqrt{\vartheta_l} &= \vartheta_l' + (\gamma'/\sqrt{\eta_1})\sqrt{\vartheta_b}\frac{\chi_0^2\tau}{\tilde\chi_l - (1/\sqrt{\eta_1})\sqrt{\vartheta_b}}\\ &\triangleq \xi_3(\vartheta_l', \vartheta_b),\end{aligned}$$

and this may be readily solved by applying the quadratic formula,

$$\sqrt{\vartheta_l} = \frac{1}{2}\left(\chi_0 + \sqrt{\chi_0^2 + 4\xi_3}\right) \triangleq \xi_4(\vartheta_l', \vartheta_b),$$

where we have discarded the second negative root.

During flight, touchdown, and next bottom, the arguments are identical to those of the previous section, and we have

$$\begin{aligned}\vartheta_{j+1} &= (\xi_4[\xi_2(\vartheta_j),\ \vartheta_j])^2\exp\left\{-\frac{2\sigma\sqrt{4\kappa-\gamma^2}}{\gamma\omega}\right\}\\ &\triangleq \tilde f(\vartheta_j).\end{aligned}$$

In principle, this case yields to the same analysis as in the previous section. It is quite clear, however, that the qualitative properties of $\tilde f$ would be considerably more difficult to determine. No attempt is made to do so in the present paper.

4 Analysis of a Simplified Nonlinear Model

In this section, we undertake an initial analysis of the nonlinear robot actuator. In so doing, we immediately encounter the limitations of the techniques of Section 3, for these require explicit integration of the underlying continuous-time dynamical system. Of course, in general, nonlinear differential equations do not admit closed form integration, and we are forced to strip away a number of crucial aspects of the model developed in Section 2.1 in order to achieve an integrable system.

After a brief discussion of the altered model and appraisal of alternative analytical techniques in Section 4.1, we will proceed with the analysis of the "stripped down" nonlinear model in Section 4.2.

4.1 Simplified Nonlinear Models and Alternative Analytical Approaches

The question naturally arises as to whether the immediate appeal to discrete dynamics is the source of difficulty. Unquestionably, certain versions of the models explored in this paper seem amenable to a qualitative analysis of the underlying continuous-time periodic orbits in the tradition of planar dynamical theory [3,2] — a body of techniques which do not require explicit integration of the vector field. However, in the face of a multiply discontinuous vector field, there are technical problems applying the standard tools. This is swiftly comprehended, for example, by a glance at the simulated trajectories of Figures 8 and 9 where the crossing of trajectories through each other belies the uniqueness of solutions. Indeed, for the models with shifting spring constant there is no single well-defined vector field at a point in the portion of the plane associated with the decompression phase. Analysis of the continuous dynamics would require passage to a phase space of higher dimension than two, and such powerful tools as the Poincaré-Bendixson Theorem would no longer be of use [3].

Therefore, consider a variation on the model 4 wherein both the environment is altered,

$$F_e \triangleq [1 - \sigma(\chi)]g,$$

to remove the viscous friction forces and the force of gravity during stance phase, and where the robot is altered by letting the time of thrust, δ_t, go to zero,

$$\eta_{nl}(\chi, \dot{\chi}, t) = \begin{cases} \eta_1 & \text{if } \dot{\chi} < 0, \chi < \chi_{td} \\ \eta_2 = \tau\chi_b & \text{if } \dot{\chi} > 0, \chi < \chi_l = \chi_{td} \\ 0 & \text{otherwise.} \end{cases}$$

Notice that this model with "instantaneous thrust phase" still incorporates the qualitatively important feature of changing the spring constant for the subseqent decompression phase. However, equation (4) can now be written as

$$\ddot{\chi} = \eta_2 \frac{1}{\chi},$$

which can be integrated easily.

In fact, on any domain where neither χ, nor $\dot{\chi}$ vanish we may either solve this system for $\dot{\chi}_1$ as a function of χ_1, and initial conditions, x_0,

$$\dot{\chi}_1^2 = 2\eta \ln \tfrac{\chi_1}{\chi_0} - \dot{\chi}_0^2, \tag{14}$$

or since this function is invertible, for χ_1 as a function of $\dot{\chi}_1$,

$$\chi_1 = \chi_0 \exp\left\{\tfrac{1}{2\eta_2}[\dot{\chi}_1^2 - \dot{\chi}_0^2]\right\}. \tag{15}$$

It is clear that both functions are well defined even when x_0 has a zero component.

4.2 Analysis of the Simplified Model

Starting at the bottom point

$$x_b = \begin{bmatrix} \chi_b \\ 0 \end{bmatrix},$$

and applying (14) gives

$$\dot{\chi}_l^2 = 2\eta_2 \ln \frac{\chi_l}{\chi_b} = 2\tau\chi_b \ln \frac{\chi_l}{\chi_b}. \tag{16}$$

Note that this map, from bottom position to liftoff velocity, is not monotone, but exhibits a maximum at $\chi = \chi_l/e$. This results in the trajectory crossing between bottom and liftoff points as which can be observed in figures 6- 10.

During flight, the hopper is subjected to a constant negative acceleration due to gravity with no losses due to friction. As liftoff and touchdown positions are identical, also the kinetic energy at liftoff and the subsequent touchdown are equivalent, and thus $\dot{\chi}_{ld}^2 = \dot{\chi}_l^2$.

From touchdown to bottom, applying (15), yields

$$\begin{aligned} \chi_{b,next} &= \chi_{ld} \exp\left\{-\tfrac{\dot{\chi}_{ld}^2}{2\eta_1}\right\} \\ &= \chi_l \exp\left\{-\tfrac{\dot{\chi}_l^2}{2\eta_1}\right\} \\ &= \chi_l \exp\left\{-\tfrac{\tau\chi_b}{\eta_1} \ln \tfrac{\chi_l}{\chi_b}\right\} \\ &\quad \text{(from (16))} \\ &= \chi_l \left(\tfrac{\chi_l}{\chi_b}\right)^{-\frac{\tau}{\eta_1}\chi_b} \\ &\triangleq f(\chi_b). \end{aligned} \tag{17}$$

Proposition 4.1 *The dynamical system (17) has a unique fixed point on the domain*

$$\mathcal{D} \triangleq (0, \chi_l).$$

Proof: From (17), equating $\chi = f(\chi)$, results in the unique solution for $\chi \in \mathcal{D}$:

$$\chi = \frac{\eta_1}{\tau} = \chi^*$$

□

It is important to note here, that the fixed point, χ^*, is explicitly given by the quotient of the two system parameters, η_1, τ, the initial spring constant during compression and the thrust force. In the sequel χ^* and $\frac{\eta_1}{\tau}$ will be used interchangeably.

Proposition 4.2 *The unique fixed point, χ^*, of (17) is locally asymptotically stable if and only if*

$$\chi^* \in \mathcal{D}_1 \triangleq (\chi_l/e^2, \chi_l).$$

Proof: A necessary and sufficient condition for the scalar difference equation (17) to be locally stable at χ^*, is that the (scalar) jacobian of the equation,

$$\frac{d}{d\chi} f = \frac{\chi_l}{\chi^*}(1 - \ln \frac{\chi_l}{\chi})(\frac{\chi_l}{\chi})^{-\frac{\chi}{\chi^*}},$$

evaluated at χ^*

$$\frac{d}{d\chi} f \mid_{\chi^*} = 1 - \ln \frac{\chi_l}{\chi^*},$$

have magnitude less than unity,

$$\left| 1 - \ln \frac{\chi_l}{\chi^*} \right| < 1,$$

leading to the conditions,

$$\chi_l/e^2 < \chi^* < \chi_l,$$

as stated.

□

This result shows that, unlike the linear case, an asymptotically stable fixed point may not be globally attracting, and, moreover, not all parameter settings give rise to even a locally attracting fixed point. Motivated by the plots in Figures 8, 10 we are led to suspect that the absence of "period-one" attractors is associated with the appearance of the more complicated double loop characteristic of a higher period orbit. This, in fact, turns out to be the case, as shown in the following result.

Proposition 4.3 *If the fixed point of (17), is not a local attractor, i.e.,*

$$\chi^* \in (0, \chi_l/e^2) \triangleq \mathcal{D}_0,$$

then there exists at least one orbit of period two, i.e. a fixed point of

$$g \triangleq f \circ f,$$

which is not a fixed point of f.

Proof: Evidently, $g(\chi^*) = \chi^*$, since a fixed point of f (a "period one" orbit) is necessarily a fixed point of every higher period orbit. Since χ^* is the unique fixed point of f, according to Proposition 4.1 , it will suffice to find conditions under which g has at least two distinct fixed points. Equivalently, defining the "ratio map",

$$r(\chi) \triangleq \frac{g(\chi)}{\chi},$$

it suffices to find two distinct unity crossings of r.

Since

$$\lim_{\chi \to 0} -\frac{\tau\chi}{\eta_1} \ln \frac{\chi_l}{\chi} = 0,$$

it follows that $\lim_{\chi \to 0} f = 1$, hence $\lim_{\chi \to 0} g$ is a bounded number, and we have

$$\lim_{\chi \to 0} r = \infty.$$

Moreover, since χ^* is a fixed point of g, we have

$$r(\chi^*) = 1.$$

Thus, it will suffice to show that

$$\frac{dr}{d\chi} |_{\chi^*} > 0,$$

for this would imply the existence of a second unity crossing of $r(\chi)$, on the interval $(0, \chi^*)$ under the conditions derived above.

This follows since

$$\begin{aligned}\frac{dg}{d\chi}\mid_{\chi^*} &= \left(\frac{g}{\chi^2}[\frac{dg}{d\chi}/r - 1]\right)\mid_{\chi^*} \\ &= \frac{r(\chi^*)}{\chi^*}[\frac{df}{d\chi}\mid_{f(\chi^*)} \cdot \frac{df}{d\chi}\mid_{\chi^*} /r(\chi^*) - 1] \\ &= \frac{1}{\chi^*}[(\frac{df}{d\chi}\mid_{\chi^*})^2 - 1] \\ &> 0,\end{aligned}$$

according to the hypothesis that χ^* is an unstable fixed point of f.

□

Combining the previous results now yields the second central contribution of this paper.

Theorem 2 *The system (6) has a unique fixed point on the domain* $\mathcal{D} \triangleq (0, \chi_l)$, *which is locally asymptotically stable if and only if* $\chi^* \in \mathcal{D}_1 \triangleq (\chi_l/e^2, \chi_l)$. *If* χ^* *is not a local attractor, i.e.,* $\chi^* \in (0, \chi_l/e^2) \triangleq \mathcal{D}_0$, *then there exists at least one orbit of period two, i.e. a fixed point of* $g \triangleq f \circ f$, *which is not a fixed point of* f.

There are obviously many more complicated behaviors that we might expect to occur in this model. Note, in particular, that we have not yet given any conditions for the stability of the period two orbit, even though its visibility in the simulations is a certain measure of local stability. However, before venturing into an analysis of these more sophisticated analytical issues, we feel that the models should be validated more carefully with regard to the underlying physical system.

Acknowledgements

We would like to acknowledge the GMF Robotics Corporation whose support, in conjunction with an NSF Presidential Young Investigator Award held by the second author, has made this research possible.

References

[1] M. Bühler and D. E. Koditschek. A prelude to juggling. In *Conference Presentation: 26th IEEE Conference on Decision and Control*, pages (paper available from authors — not in proceedings), Los Angeles, CA, Dec. 1987.

[2] D. E. Koditschek and K. S. Narendra. Limit cycles of planar quadratic systems. *Journal of Differential Equations*, (2).

[3] Solomon Lefschetz. *Differential Equations: Geometric Theory.* Dover, NY, 1977.

[4] D. E. Koditschek and M. Bühler. Distributed Control System for a Juggling Robot. In *Oregon State University Conference on Parallel Processing*, Oregon State University, Portland, OR, Apr 1988.

[5] Marc H. Raibert. *Legged Robots That Balance.* MIT Press, Cambridge, MA, 1986.